

A Set of Molecular Models for Symmetric Quadrupolar Fluids

Jadran Vrabec,* Jürgen Stoll, and Hans Hasse

Institut für Technische Thermodynamik und Thermische Verfahrenstechnik, Universität Stuttgart, D-70550 Stuttgart, Germany

Received: July 5, 2001; In Final Form: September 11, 2001

Molecular models for 25 different pure fluids are presented: neon, argon, krypton, xenon, methane, oxygen, nitrogen, fluorine, chlorine, bromine, iodine, carbon dioxide, carbon disulfide, ethane, ethene, ethyne, perfluoroethane, perfluoroethene, perchloroethene, propadiene, propyne, sulfurhexafluoride, tetrafluoromethane, tetrachloromethane, and propylene. The models are based on the two-center Lennard-Jones plus pointquadrupole pair potential (2CLJQ). The model parameters were adjusted to experimental vapor–liquid equilibria of the pure fluids using a highly efficient procedure. The application of these models to the calculation of vapor–liquid equilibria and homogeneous fluid state points by molecular simulation shows good agreement with experimental results. Numbers for model parameters correlate reasonably with geometric data of the molecules and experimental quadrupole moments. Due to the compatibility of the presented models, applications to the prediction of vapor–liquid equilibria of mixtures are straightforward.

Introduction

In chemical and thermal process engineering, knowledge of vapor–liquid equilibria (VLE) of pure substances and mixtures is essential. Conventional methods for the calculation of VLE, equations of state and G^E models, are excellent correlation tools but often lack in predictive power. This shortcoming is due to the insufficient physical basis of the conventional methods.

In recent years, the availability of more and more powerful computers has opened the route to obtaining VLE from molecular models by direct numerical simulation as an alternative to the conventional methods. Molecular simulation relates macroscopic thermodynamic phenomena to their roots in molecular interactions. This description of molecular interactions can yield physically meaningful models of excellent predictive power.¹

The practical applicability of molecular simulations in process engineering requires appropriate molecular models for real fluids. The molecular models of the individual fluids must accurately describe thermodynamic data of the pure fluids. The structure of the molecular models has to be as simple as possible in order to keep the number of model parameters low. This leads to easier extension to mixtures and generally better predictive power of the model. Furthermore, simplicity of the models reduces the computation time. Finally, with regard to simulations of fluid mixtures, a family of compatible molecular models has to be used.

In this work, we present state independent molecular models for 25 real fluids (cf. Table 1) on the basis of the two-center Lennard-Jones plus pointquadrupole pair potential (2CLJQ), which accurately describe the thermodynamic properties of the fluids. Typical relative deviations of simulation results and experiment are $\pm 3\%$ for the vapor pressure, $\pm 0.5\%$ for the saturated liquid density, and $\pm 2\%$ for the enthalpy of vaporization.

The time required for the development of new molecular models for many symmetric quadrupolar real fluids was

considerably reduced, as a new route was followed by applying global correlations, that describe the VLE of the 2CLJQ model fluid in terms of its molecular parameters.² These global correlations are used to adjust the 2CLJQ model parameters efficiently to VLE data of the 25 real fluids.

For the symmetric quadrupolar fluids considered here, numerous molecular models have been published by other authors, Ne,^{3–5} Ar,^{3–9} Kr and Xe,^{3,4,7,10} CH₄,^{6–8,11–13} O₂,^{4,14–16} N₂,^{4,6,16–19} F₂,^{6,17} Cl₂,^{14,16,17,20–23} Br₂,^{14,17,24} CO₂,^{4,6,7,17,25–30} CS₂,^{4,14,31} C₂H₆,^{6,7,11–13,16,27,32,33} C₂H₄,^{14,34} C₂H₂,^{7,34} CF₃CF₃,¹⁶ CF₂CF₂,¹⁶ CF₄,^{35,36} CCl₄,^{6,37,38} However, for several reasons, many of these models are not appropriate for the calculation of VLE of the pure fluid and fluid mixtures. Some of the available molecular models are designed for other applications, such as liquid or solid simulations with investigations of structure^{4,9,17,24–26,35,37,38} or the description of the second virial coefficient,³ and often yield poor results when applied to VLE. Many of the models are incompatible as different types of models are used: Kihara-,^{16,29} exponential-6-,³³ Lennard-Jones- n -6-,⁶ or very specialized potentials with a large number of parameters.^{5,20–22} In contrast, the present 2CLJQ potential models are compatible and are all designed for simulations of VLE.

In section 2 we concisely describe the 2CLJQ potential model and give an outline of the procedure applied to determine the 2CLJQ model parameters. In section 3 the results of applications of these molecular models are presented and compared to experimental data. The paper closes with physical interpretations of the potential parameters.

2. Model Fluids, Procedure

The symmetrical two-center Lennard-Jones plus pointquadrupole pair potential (2CLJQ) is a powerful model for the pair interactions of symmetrical, unpolar, or quadrupolar molecules. The 2CLJQ potential is composed of two identical Lennard-Jones (LJ) sites a distance L apart (2CLJ) plus a pointquadrupole of moment Q placed in the geometric center of the molecule:

$$u_{2CLJQ}(\mathbf{r}_{ij}, \omega_i, \omega_j, L, Q) = u_{2CLJ}(\mathbf{r}_{ij}, \omega_i, \omega_j, L) + u_Q(\mathbf{r}_{ij}, \omega_i, \omega_j, Q) \quad (1)$$

* Author for correspondence, Tel.: ++49-711/685-6107, Fax: ++49-711/685-7657, E-mail: vrabec@itt.uni-stuttgart.de.

TABLE 1: Potential Model Parameters for 25 Pure Substances Determined in the Present Work

fluid	$\sigma/\text{\AA}$	$(\epsilon/k_B)/K$	$L/\text{\AA}$	$Q/D\text{\AA}$	fluid	$\sigma/\text{\AA}$	$(\epsilon/k_B)/K$	$L/\text{\AA}$	$Q/D\text{\AA}$
Ne	2.8010	33.921		0	C ₂ H ₆	3.4896	136.99	2.3762	0.8277
Ar	3.3952	116.79		0	C ₂ H ₄	3.7607	76.950	1.2695	4.3310
Kr	3.6274	162.58		0	C ₂ H ₂	3.5742	79.890	1.2998	5.0730
Xe	3.9011	227.55		0	C ₂ F ₆	4.1282	110.19	2.7246	8.4943
CH ₄	3.7281	148.55		0	C ₂ F ₄	3.8611	106.32	2.2394	7.0332
F ₂	2.8258	52.147	1.4129	0.8920	C ₂ Cl ₄	4.6758	211.11	2.6520	16.143
Cl ₂	3.4016	160.86	1.9819	4.2356	propadiene	3.6367	170.52	2.4958	5.1637
Br ₂	3.5546	236.76	2.1777	4.8954	propyne	3.5460	186.43	2.8368	5.7548
I ₂	3.7200	371.47	2.6784	5.6556	SF ₆	3.9615	118.98	2.6375	8.0066
N ₂	3.3211	34.897	1.0464	1.4397	CF ₄	3.8812	59.235	1.3901	5.1763
O ₂	3.1062	43.183	0.9699	0.8081	CCl ₄	4.8471	142.14	1.6946	14.346
CO ₂	2.9847	133.22	2.4176	3.7938	propylene	3.8169	150.78	2.5014	5.9387
CS ₂	3.6140	257.68	2.6809	3.8997					

wherein

$$u_{2\text{CLJ}}(\mathbf{r}_{ij}, \omega_i, \omega_j, L) = \sum_{a=1}^2 \sum_{b=1}^2 4\epsilon \left[\left(\frac{\sigma}{r_{ab}} \right)^{12} - \left(\frac{\sigma}{r_{ab}} \right)^6 \right] \quad (2)$$

and

$$u_Q(\mathbf{r}_{ij}, \omega_i, \omega_j, Q^2) = \frac{3}{4} \frac{Q^2}{|\mathbf{r}_{ij}|^5} f(\omega_i, \omega_j) \quad (3)$$

The pointquadrupole used here represents an arrangement of charges $+-+ -$ or, having the same energetic effect in pure fluids, $-++ -$, along the molecular axis. This charge distribution typically occurs in the fluids investigated here. Thus the function $f(\omega_i, \omega_j)$ depends only on the orientations ω_i and ω_j of two interacting molecules i and j . It is given by Gray et al.³⁹ The vector \mathbf{r}_{ij} indicates the center-center distance of the two molecules, r_{ab} is one of the four LJ site-site distances; a counts the two sites of molecule i , b counts those of molecule j . The LJ parameters σ and ϵ represent size and energy, respectively. In molecular simulations of LJ-based fluids, typically all thermodynamic properties are scaled to σ and ϵ , i.e., here temperature $T^* = T k_B / \epsilon$ (k_B is the Boltzmann constant), pressure $p^* = p \sigma^3 / \epsilon$, density $\rho^* = \rho \sigma^3$, enthalpy $h^* = h / \epsilon$, but also the elongation $L^* = L / \epsilon$ and the squared quadrupole moment $Q^{*2} = Q^2 / (\epsilon \sigma^5)$.

The 2CLJQ potential model explicitly takes into account the shape and polarity of the molecule. The LJ sites can be used to model the van der Waals interactions of both single atoms or groups of bonded atoms.

In the present work, only pairwise additive interactions are considered, as no essential improvements can be expected from taking into account multibody interactions.⁴⁰

The fluids modeled can be grouped as follows:

Spherical. This group contains the monatomic noble gases neon (Ne), argon (Ar), krypton (Kr), and xenon (Xe), and also methane (CH₄). For these fluids, new sets of LJ parameters are given here, as the 2CLJQ model comprises the spherical LJ model.

Symmetric Diatomic. This group contains oxygen (O₂), nitrogen (N₂), and the halogens fluorine (F₂), chlorine (Cl₂), bromine (Br₂), and iodine (I₂). Each atom is modeled by a LJ site.

Symmetric Triatomic. A simplifying but successful approach to model the interactions of three bonded atoms is to condense them to two LJ sites. The elongation L of the 2CLJQ model fluid then models the elongated shape of carbon dioxide (CO₂) and carbon disulfide (CS₂).

C₂ Derivative. This group comprises molecules based on two carbon atoms with a single, double, or triple bond, i.e., ethane

(C₂H₆), ethene (C₂H₄), ethyne (C₂H₂), perfluoroethane (C₂F₆), perfluoroethene (C₂F₄), and perchloroethene (C₂Cl₄).

Linear C₃ Derivative. Propadiene (C₃H₄) and propyne (C₃H₄) comprise this group. Propyne's slightly asymmetric shape and its weak dipole moment of about 0.7 D⁴¹ in the gas state are neglected here.

Test Cases. This group includes tetrafluoromethane (CF₄), tetrachloromethane (CCl₄), sulfurhexafluoride (SF₆), and propylene (C₃H₆), whose weak dipole moment of about 0.4 D⁴¹ in the gas state is neglected. These fluids have been modeled due to their geometry, which can be approached by the shape of the 2CLJQ model fluids. However, as SF₆ is hexadecapolar and CF₄ and CCl₄ are intensively octopolar due to the distinct polarity of the CF- and the CCl- bonds, the parameters Q and L will degenerate to pure fit parameters. The bonding angle of propylene is not modeled explicitly.

It is known that molecular models, which have been fitted to experimental vapor-liquid equilibria, are able to describe thermophysical properties in the whole fluid state region with good accuracy.²⁸ In the present work, we develop state independent molecular models by applying the correlations from Stoll et al.² for the reduced critical temperatures $T_c^*(Q^{*2}, L^*)$, the reduced saturated liquid densities $\rho'^*(Q^{*2}, L^*, T^*)$, and the reduced vapor pressures $p_\sigma^*(Q^{*2}, L^*, T^*)$ of the 2CLJQ model fluid when fitting the 2CLJQ model parameters to experimental critical temperatures T_c , saturated liquid densities ρ' , and vapor pressures p_σ . According to our experience, the inclusion of ρ' and p_σ in the adjustment procedure ensures, that the molecular models also describe the enthalpies h with good accuracy. So good predictions of enthalpies of vaporization ΔH_v may be expected.

To include eventual temperature dependent effects, we used various data points on the vapor-liquid coexistence curves between about 0.55 T_c up to about 0.95 T_c in the fitting procedure. With the aforementioned correlations from Stoll et al.,² the underlying optimization equations for the relative deviations are

$$(T_c^*(Q^{*2}, L^*) \epsilon / k_B - T_{c,\text{exp}}) / T_{c,\text{exp}} \stackrel{!}{=} \min \quad (4)$$

$$\sum_i [(p_\sigma^*(Q^{*2}, L^*, T_i k_B / \epsilon) / \sigma^3 - p_{\sigma,\text{exp}}(T_i)) / p_{\sigma,\text{exp}}(T_i)] \stackrel{!}{=} \min \quad (5)$$

$$\sum_i [(\rho'^*(Q^{*2}, L^*, T_i k_B / \epsilon) / \sigma^3 - \rho'_{\text{exp}}(T_i)) / \rho'_{\text{exp}}(T_i)] \stackrel{!}{=} \min \quad (6)$$

Herein, i counts the data points at different temperatures T_i . The adjustment of LJ parameters for the group of spherical fluids was carried out with the correlations for $p_\sigma^*(T^*)$ and $\rho'^*(T^*)$ from Lotfi et al.⁴² for the VLE of the spherical LJ fluid, as these correlations yield slightly better results than do the correlations from Stoll et al.² for $Q^{*2} = 0$, $L^* = 0$.

TABLE 2: Database Used in the Present Work

fluid	p_σ	$\rho\phi$	ΔH_v	fluid	p_σ	$\rho\phi$	ΔH_v
Ne	[43]	[44]	[45]	C ₂ H ₆	[54]	[54]	[54]
Ar	[46]	[46]	[46]	C ₂ H ₄	[55]	[55]	[55]
Kr	[45]	[44]	[45]	C ₂ H ₂	[56]	[45]	[45]
Xe	[45]	[44]	[45]	C ₂ F ₆	[57]	[57]	[57]
CH ₄	[47]	[47]	[47]	C ₂ F ₄	[48]	[45]	[45]
F ₂	[43]	[44]	[45]	C ₂ Cl ₄	[48]	[45]	[45]
Cl ₂	[48]	[44]	[45]	propadiene	[45]	[44]	[45]
Br ₂	[45]	[49]	[45]	propyne	[48]	[44]	[45]
I ₂	[45]	[44]	[45]	SF ₆	[45]	[45]	[45]
N ₂	[50]	[50]	[50]	CF ₄	[58]	[58]	[58]
O ₂	[51]	[51]	[51]	CCl ₄	[43]	[45]	[59]
CO ₂	[52]	[52]	[52]	propylene	[60]	[60]	[60]
CS ₂	[45]	[45]	[53]				

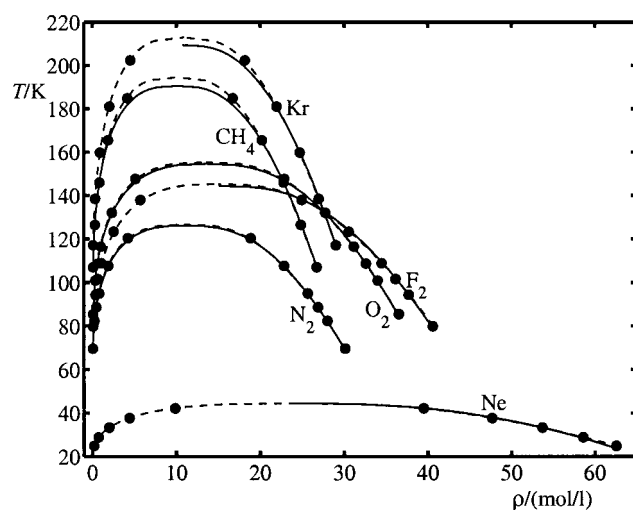


Figure 1. Comparison I of saturated densities from simulation (●) and correlations from Stoll et al.² (---) to experimental data (—). Error bars are, if not indicated, within symbol size. (Experimental data cf. Table 2.)

Numbers for experimental data $p_{\sigma,\text{exp}}(T_i)$ and $\rho'_{\text{exp}}(T_i)$ in eqs 5 and 6 were taken from correlations of experimental data of vapor pressures p_σ and saturated liquid densities ρ' available in the references given in Table 2. With respect to the statistical uncertainties of the molecular simulations, we assume these correlations of experimental data to be exact. Experimental critical temperatures $T_{c,\text{exp}}$ are taken from ref 48.

In many cases, the nonlinear optimization directly led to physically meaningful parameter sets. In other cases, the solution space for the reduced parameters Q^{*2} and L^* was limited in order to ensure physically reasonable solutions.

Table 1 gives the parameters for the 2CLJQ models for all fluids studied in the present work. We indicate absolute values of the parameter Q , calculated as $|Q^*|(4\pi\epsilon_0\epsilon\sigma^5)^{1/2} \cdot 2.9979 \times 10^{39} \text{ D}\text{\AA}$,³⁹ wherein $\epsilon_0 = 8.85419 \times 10^{-12} \text{ C}^2/(\text{Nm}^2)$ is the permittivity of the vacuum.

3. Results for Thermodynamic Properties

Molecular simulations of VLE were carried out with the NpT +Test Particle method.^{61,62} Moreover, molecular simulations of various homogeneous fluid state points were performed in the NpT ensemble. Technical details of the simulations were identical to those given in ref 2. Figures 1–4 compare the saturated densities, Figures 5–8 the vapor pressures, and Figures 9–12 the enthalpies of vaporization of the present molecular models to experimental data. (The grouping of fluids in Figures 1–12 is subject to graphical requirements.) For CS₂ and CCl₄,

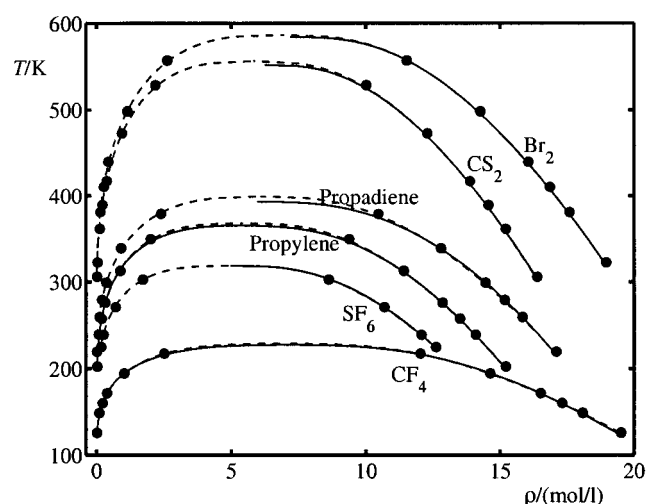


Figure 2. Comparison II of saturated densities from simulation (●) and correlations from Stoll et al.² (---) to experimental data (—). Error bars are, if not indicated, within symbol size. (Experimental data cf. Table 2.)

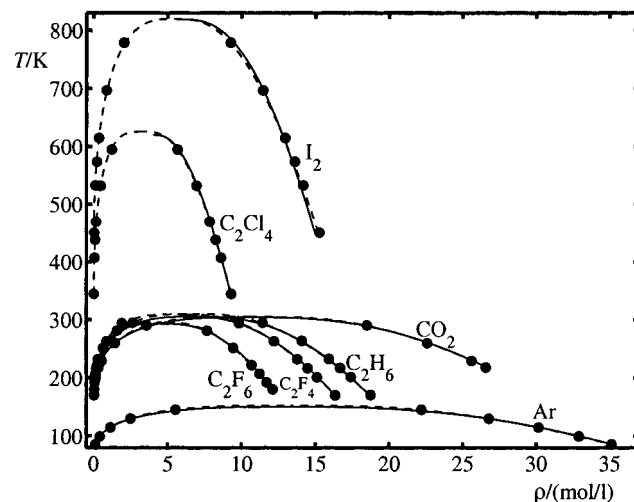


Figure 3. Comparison III of saturated densities from simulation (●) and correlations from Stoll et al.² (---) to experimental data (—). Error bars are, if not indicated, within symbol size. (Experimental data cf. Table 2.)

experimental data for the enthalpies of vaporization are only available in a small temperature range.

For the saturated liquid densities, for almost all fluids modeled here, the relative deviations of the simulation results to experimental data $|\delta\rho'| = |(\rho'_{\text{sim}} - \rho'_{\text{exp}})/\rho'_{\text{exp}}|$ are clearly below 1%. For temperatures around $0.7T_c$, the relative deviations of the vapor pressures $|\delta p_\sigma| = |(p_\sigma - p_{\sigma,\text{exp}})/p_{\sigma,\text{exp}}|$ are about $\pm 3\%$ or less (e.g., C₂H₆, F₂, Cl₂, Br₂, or I₂). For temperatures above about $0.85T_c$ and below about $0.65T_c$, relative deviations of the vapor pressures increase to about $\pm 5\%$. This is due to the increasing influence of critical effects and to the uncertain calculation of the chemical potential in dense phases by Widom's test particle method. Moreover, most of the molecular models predict the enthalpies of vaporization also very well, although the model parameters were not adjusted to this type of data. Typically, they have relative deviations $|\delta\Delta H_v| = |(\Delta H_{v,\text{sim}} - \Delta H_{v,\text{exp}})/\Delta H_{v,\text{exp}}|$ below 3%, in many cases even below 1% (e.g., C₂H₆, C₂F₄, C₂F₆, I₂, or O₂). Deviations increase for state points close to the critical point, as the critical temperature given by the molecular models tends in most cases to be slightly higher than the experimental number.

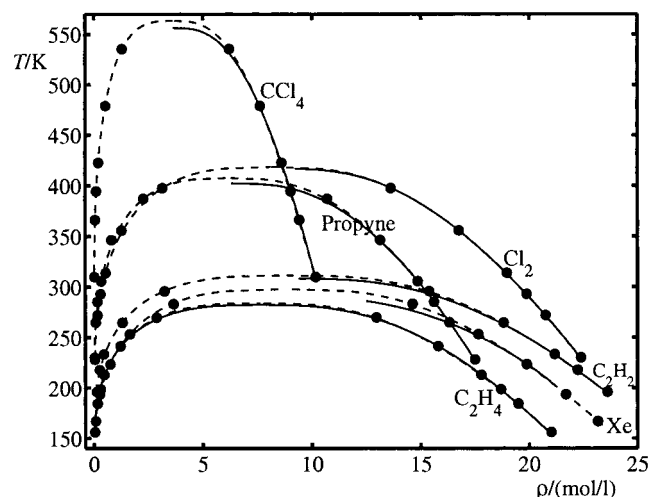


Figure 4. Comparison IV of saturated densities from simulation (●) and correlations from Stoll et al.² (---) to experimental data (—). Error bars are, if not indicated, within symbol size. (Experimental data cf. Table 2.)

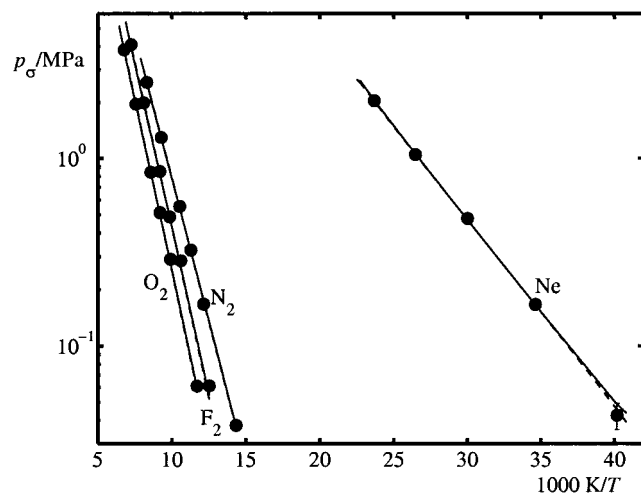


Figure 5. Comparison I of vapor pressures from simulation (●) and correlations from Stoll et al.² (---) to experimental data (—). (Experimental data cf. Table 2.)

Even the results for the test case fluids are surprisingly good. However, the molecular models for the test case fluids have to be treated cautiously for the reasons stated above.

In Table 3 experimental data of the critical temperature T_c , critical pressure p_c , critical density ρ_c , and critical compressibility

$$Z_c = \frac{p_c}{\rho_c RT_c} \quad (7)$$

as well as the acentric factor

$$\omega = -\log_{10}\left(\frac{p_\sigma(0.7T_c)}{p_c}\right) - 1 \quad (8)$$

are compared to the results from the present molecular models using results of the correlations from Stoll et al.² Typical relative deviations between the critical data obtained from the molecular models and experimental numbers are about 4% for p_c and 1–2% for ρ_c . It can be seen from Table 3 that the reduced properties Z_c and ω for the LJ models are all equal but generally agree fairly well with the experimental data.

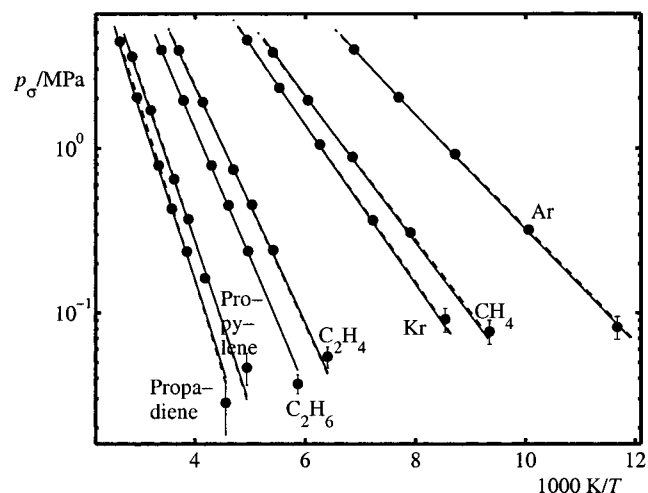


Figure 6. Comparison II of vapor pressures from simulation (●) and correlations from Stoll et al.² (---) to experimental data (—). (Experimental data cf. Table 2.)

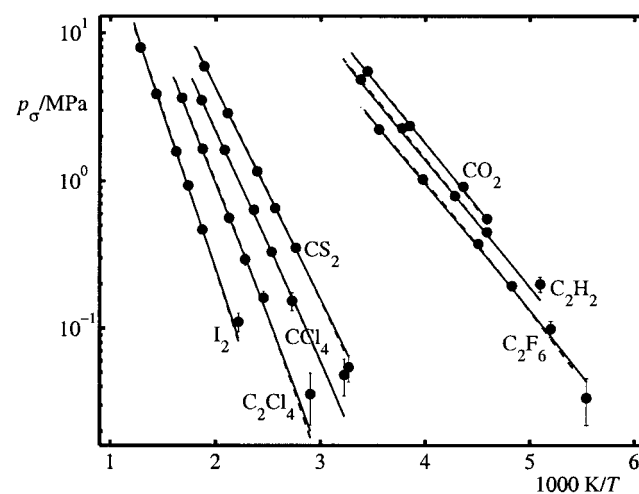


Figure 7. Comparison III of vapor pressures from simulation (●) and correlations from Stoll et al.² (---) to experimental data (—). (Experimental data cf. Table 2.)

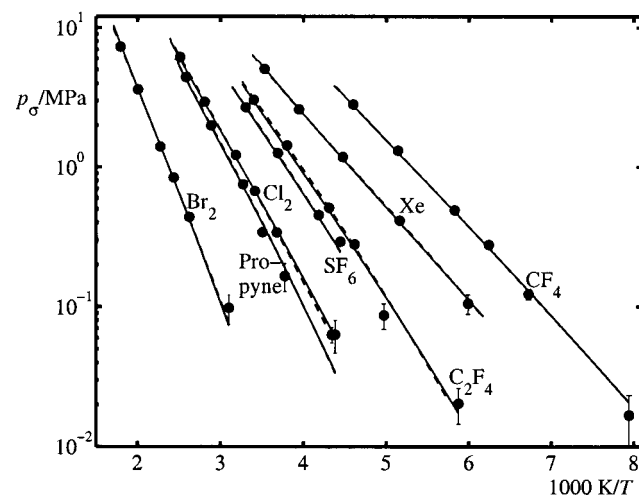
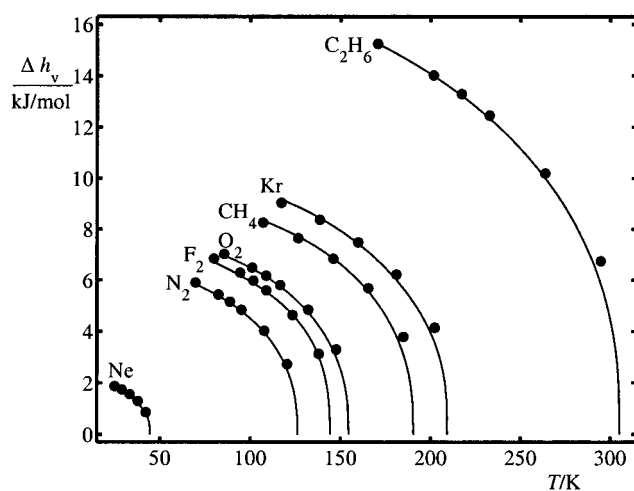


Figure 8. Comparison IV of vapor pressures from simulation (●) and correlations from Stoll et al.² (---) to experimental data (—). (Experimental data cf. Table 2.)

Figures 1–12 as well as Table 3 show, that the present molecular models allow accurate simulation of VLE of the pure fluids considered here.

TABLE 3: Critical Properties and Acentric Factors from the Present Molecular Models in Comparison to Experimental Data⁴⁸

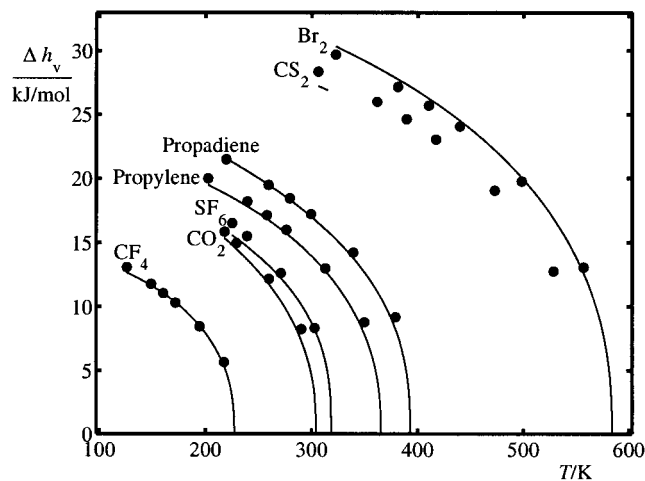
fluid		T_c/K	p_c/MPa	$r_c/mol/L$	Z_c	ω	fluid		T_c/K	p_c/MPa	$r_c/mol/L$	Z_c	ω
Ne	exp.	44.4	2.76	24.04	0.311	-0.029	C ₂ H ₆	exp.	305.4	4.88	6.74	0.285	0.099
	mod.	44.4	2.69	23.72	0.306	-0.032		mod.	310.2	5.27	6.74	0.303	0.065
Ar	exp.	150.8	4.87	13.35	0.291	0.001	C ₂ H ₄	exp.	282.4	5.04	7.67	0.280	0.089
	mod.	153.0	5.21	13.32	0.306	-0.032		mod.	284.0	5.29	7.62	0.294	0.091
Kr	exp.	209.4	5.50	10.96	0.288	0.005	C ₂ H ₂	exp.	308.3	6.14	8.87	0.270	0.190
	mod.	213.0	5.94	10.92	0.306	-0.032		mod.	311.4	6.67	8.88	0.290	0.186
Xe	exp.	289.7	5.84	8.45	0.287	0.008	C ₂ F ₆	exp.	293.0	3.06	4.50	0.279	
	mod.	298.1	6.69	8.78	0.306	-0.032		mod.	296.0	3.15	4.41	0.290	0.227
CH ₄	exp.	190.4	4.60	10.08	0.288	0.011	C ₂ F ₄	exp.	306.5	3.94	5.81	0.267	0.223
	mod.	194.6	5.00	10.06	0.306	-0.032		mod.	309.5	4.36	5.75	0.295	0.210
F ₂	exp.	144.3	5.22	15.08	0.288	0.054	C ₂ Cl ₄	exp.	620.2	4.76	3.45	0.250	
	mod.	145.2	5.44	15.05	0.300	0.050		mod.	626.2	5.02	3.27	0.294	0.212
Cl ₂	exp.	416.9	7.98	8.08	0.285	0.090	propadiene	exp.	393.	5.47	6.17	0.271	0.313
	mod.	418.6	8.39	8.10	0.297	0.100		mod.	399.	5.94	6.08	0.295	0.121
Br ₂	exp.	588.	10.3	7.86	0.268	0.108	propyne	exp.	402.4	5.63	6.10	0.275	0.215
	mod.	587.	10.0	6.86	0.298	0.086		mod.	407.6	5.96	6.18	0.285	0.174
I ₂	exp.	819.	11.73 ^a	6.45			SF ₆	exp.	318.7	3.76	5.03	0.282	0.286
	mod.	820.	11.12	5.44	0.300	0.087		mod.	318.7	3.82	4.97	0.290	0.231
N ₂	exp.	126.2	3.39	11.14	0.290	0.039	CF ₄	exp.	227.6	3.74	7.16	0.276	0.177
	mod.	126.7	3.46	11.13	0.295	0.034		mod.	228.9	3.85	6.94	0.291	0.169
O ₂	exp.	154.6	5.04	13.62	0.288	0.025	CCl ₄	exp.	556.4	4.56	3.62	0.272	0.193
	mod.	155.4	5.18	13.58	0.295	0.018		mod.	563.6	4.91	3.61	0.290	0.179
CO ₂	exp.	304.1	7.38	10.65	0.274	0.239	propylene	exp.	364.9	4.60	5.52	0.274	0.144
	mod.	305.6	7.49	10.55	0.279	0.232		mod.	368.1	4.90	5.43	0.295	0.129
CS ₂	exp.	552.	7.90	6.25	0.276	0.109							
	mod.	556.	8.13	5.83	0.302	0.083							

^a Value is taken from ref 63.**Figure 9.** Comparison I of enthalpies of vaporization from simulation (●) to experimental data (—). Error bars are, if not indicated, within symbol size. (Experimental data cf. Table 2.)

Apart from simulations of VLE, the molecular models developed in the present work were used at various homogeneous fluid state points. In Table 4 typical results of these simulations are compared to experimental data of density ρ and residual enthalpy $H^{\text{res}}(T, p) = H(T, p) - H^{\text{ideal gas}}(T)$. Also, data points far from the vapor–liquid equilibrium region are included in the comparison. In most cases densities from the simulation agree very well with the experimental data. Residual enthalpies are also reasonably predicted. Relative deviations $|\delta H^{\text{res}}| = |(H_{\text{sim}}^{\text{res}} - H_{\text{exp}}^{\text{res}})/H_{\text{exp}}^{\text{res}}|$ are typically about 3%. These results demonstrate the good predictive power of molecular models adjusted to VLE data.

4. Discussion

The parameters of the molecular models developed in the present work were adjusted to vapor–liquid equilibrium data only. No direct information on quadrupole moments or molecule

**Figure 10.** Comparison II of enthalpies of vaporization from simulation (●) to experimental data (—). Error bars are, if not indicated, within symbol size. (Experimental data cf. Table 2.)

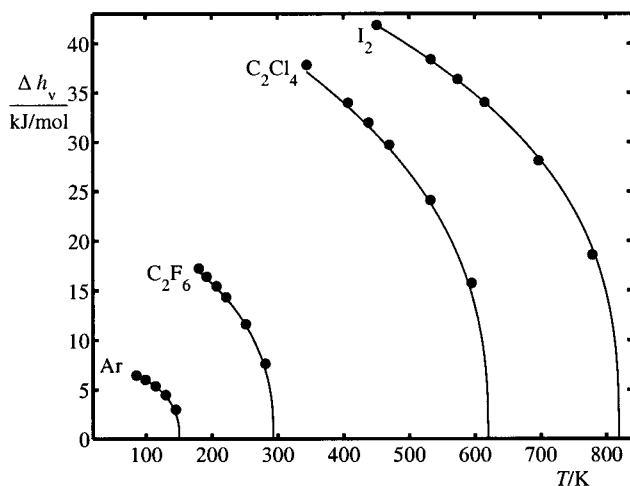
geometry was included. It is therefore interesting to compare the results for the parameters Q and L to experimental data of quadrupole moments and atom–atom distances, cf. Tables 5 and 6.

For the symmetric diatomics F₂, Cl₂, Br₂, I₂, O₂, and N₂, the parameter Q is within the range of experimental quadrupole moments and, except for O₂, the parameter L agrees within 5% of the experimental atom–atom distances. The parameter Q obtained for CO₂, CS₂, C₂H₂, and propadiene is also in the range of the different numbers reported for the experimental quadrupole moment. In the case of C₂H₄, the parameter Q is only about 8% higher than the largest value of the experimental quadrupole moment.

If ethane, which is a particular case, is omitted, the experimental geometries of the fluids in the symmetric triatomic, C₂ derivative, and linear C₃ derivative classes may conveniently be compared to values of the parameter L . For this purpose, average atom–atom distances are considered. For example, the

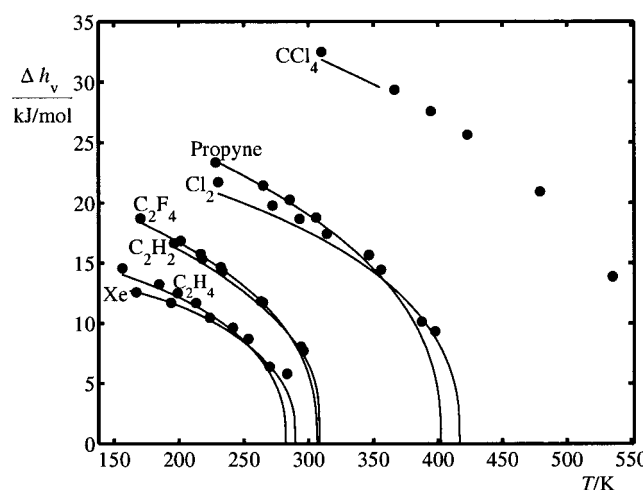
TABLE 4: Results from NpT Simulations with Present Molecular Models of Various Homogeneous Fluid State Points and Comparison to Experimental Data^a

fluid	T/K	p_o/MPa		$\rho/\text{mol/L}$	$H^{\text{res}}/\text{J/mol}$	fluid	T/K	p_o/MPa		$\rho/\text{mol/L}$	$H^{\text{res}}/\text{J/mol}$
C_2F_6	222	0.1	exp.	0.056	−214	N_2	95	0.2	exp.	0.266	−103
			sim.	0.057(1)	−205(3)				sim.	0.2647(9)	−96(2)
	222	7	exp.	11.046	−14849		95	7	exp.	26.60	−5045
			sim.	11.008(3)	−14787(8)				sim.	26.64(1)	−5055(3)
	222	20	exp.	11.489	−14339		95	20	exp.	27.99	−4816
			sim.	11.487(5)	−14303(8)				sim.	27.99(1)	−4827(2)
	423	2.845	exp.	0.882	−1215		280	5.198	exp.	2.260	−355
			sim.	0.876(2)	−1196(8)				sim.	2.255(2)	−343(3)
	423	7.393	exp.	2.52	−3316		280	14.930	exp.	6.360	−882
			sim.	2.520(5)	−3169(11)				sim.	6.317(5)	−846(3)
	423	49.551	exp.	8.5	−6653		280	114.92	exp.	22.26	−138
			sim.	8.543(5)	−6339(9)				sim.	22.08(1)	−109(3)
C_2H_4	213	0.3	exp.	0.178	−260	CO_2	260	1.2	exp.	0.618	−749
			sim.	0.177(1)	−220(10)				sim.	0.612(3)	−648(8)
	213	10	exp.	18.410	−11978		260	10	exp.	23.52	−13558
			sim.	18.385(8)	−12151(58)				sim.	23.30(2)	−13809(13)
	213	20	exp.	18.914	−11748		260	20	exp.	24.31	−13544
			sim.	18.889(7)	−11942(5)				sim.	24.04(2)	−13809(11)
	450	5.311	exp.	1.524	−1136		550	99.98	exp.	16.08	−4623
			sim.	1.511(2)	−1010(6)				sim.	15.44(1)	−4464(11)
	450	13.95	exp.	4.354	−2908		600	10.3	exp.	2.110	−954
			sim.	4.260(7)	−2642(9)				sim.	2.088(4)	−887(10)
	450	171.51	exp.	17.6	−2651		600	29.74	exp.	6.029	−2420
			sim.	17.379(5)	−2410(6)				sim.	5.846(6)	−2221(9)

^a Numbers in parentheses are uncertainties of the last digits.**Figure 11.** Comparison III of enthalpies of vaporization from simulation (●) to experimental data (—). Error bars are, if not indicated, within symbol size. (Experimental data cf. Table 2.)

distance of the sulfur atoms in CS_2 is about $2 \times 1.56 \text{ \AA} = 3.12 \text{ \AA}$,⁶⁶ cf. top of Figure 13. The parameter $L = 2.6809 \text{ \AA}$ of CS_2 has to be smaller than the sulfur–sulfur distance, as each of the LJ-sites in the 2CLJQ model has to account for one sulfur atom but also for “half” a carbon atom. In the case of C_2H_2 , the carbon–carbon distance of 1.36 \AA ⁶⁶ is close to its parameter $L = 1.30 \text{ \AA}$. For the C_2 derivatives containing F or Cl, similar considerations are possible. For example, by basic geometric calculations (cf. bottom of Figure 13) the average elongation of C_2F_4 can be estimated to $|\text{C} = \text{C}| + |\text{C} - \text{F}| \cos(\angle \text{FCF}/2) = 1.31 \text{ \AA} + 1.31 \text{ \AA} \cos(114.5^\circ/2) = 2.02 \text{ \AA}$,⁶⁶ which compares fairly well to its parameter $L = 2.2394 \text{ \AA}$. In these reflections, carbon–hydrogen distances are not regarded but carbon–halogen distances are taken into account, as the influence of bonded hydrogen atoms on the position of LJ-sites can be neglected, whereas the influence of bonded halogen atoms is remarkable.

For ethane, an acceptable description of the VLE could only be obtained when high numbers for either the parameter Q or

**Figure 12.** Comparison IV of enthalpies of vaporization from simulation (●) to experimental data (—). Error bars are, if not indicated, within symbol size. (Experimental data cf. Table 2.)

the parameter L were accepted. The stiff 2CLJQ potential model has no internal degrees of freedom and needs these increases in order to compensate for the energy stored in conformation changes of the methyl groups in real ethane molecules, which substantially influence the thermodynamics of fluid ethane. Here, we decided to accept a high number for the parameter L , thus transforming mechanical energy of internal conformation changes to mechanical energy of external rotation of the molecule. The present parameter $L = 2.3762 \text{ \AA}$ of ethane is considerably larger than the experimental carbon–carbon distance of 1.55 \AA .⁶⁶ However, the parameter Q is in agreement with the experimental quadrupole moment within the experimental uncertainty.

In the following, a brief discussion of the physical interpretation of the size parameters σ and the energy parameters ϵ is given. Generally, for larger groups of bonded atoms in molecules larger numbers for σ can be expected, as is seen by a comparison of the size parameters σ of C_2H_4 , C_2F_4 , and C_2F_6 , cf. Table 1. In the case of the noble gases Ne, Ar, Kr, and Xe or the halogens F_2 , Cl_2 , Br_2 , and I_2 the numbers for σ increase with the molecular

TABLE 5: Comparison of the Model Parameter Q to Experimental Data for the Quadrupole Moment Q_{exp}^a

fluid	$ Q_{\text{exp}} /\text{D}\text{\AA}$	$Q/\text{D}\text{\AA}$
F ₂	0.45–1.5 ^b	0.89
Cl ₂	3.23–5.5 ^b	4.24
Br ₂	4.78 ^b	4.90
I ₂	5.61 ^b	5.66
N ₂	1.39–1.6 ^b , 0.8–2.05 ^c	1.44
O ₂	0.4 ^b , 0.32–1.90 ^c	0.81
CO ₂	1.64–4.87 ^b , 2.5–5.9 ^c	3.79
CS ₂	1.8–6.8 ^b	3.90
C ₂ H ₆	0.41–3.2 ^b , 0.3–0.75 ^c	0.83
C ₂ H ₄	3.05–3.90 ^b , 1.3–4.0 ^c	4.33
C ₂ H ₂	3.0–8.4 ^b	5.07
propadiene	4.17–7.3 ^b	5.16

^a For C₂H₄, Gray³⁹ indicates values of the diagonal matrix elements Q_{xx} , Q_{yy} , and Q_{zz} of the quadrupole tensor, which have been transformed here to the effective quadrupole moment through $Q_{\text{exp}}^2 = 2/3(Q_{xx}^2 + Q_{yy}^2 + Q_{zz}^2)$, as proposed by Eubank.⁶⁵ ^b Taken from Gray.³⁹ ^c Taken from Wendland.⁶⁴

TABLE 6: Comparison of the Model Parameter L to Experimental Data for Atom–Atom Distances L_{exp}

fluid	atom–atom distances $L_{\text{exp}}/\text{\AA}$	$L/\text{\AA}$
F ₂	F–F: 1.435 ^a	1.413
Cl ₂	Cl–Cl: 2.00 ^a	1.982
Br ₂	Br–Br: 2.28 ^a	2.178
I ₂	I–I: 2.66 ^a	2.678
N ₂	N≡N: 1.0975 ^b	1.046
O ₂	O–O: 1.208 ^b	0.970
CO ₂	C=O: 1.15 ^a	2.418
CS ₂	C=S: 1.56 ^a	2.681
C ₂ H ₆	C–C: 1.55, C–H: 1.09 ^a	2.376
C ₂ H ₄	C=C: 1.33, C–H: 1.06 ^a	1.269
C ₂ H ₂	C≡C: 1.205, C–H: 1.06 ^a	1.300
C ₂ F ₆	C–C: 1.57, C–F: 1.36, bond angle FCF: 108° ^a	2.725
C ₂ F ₄	C=C: 1.31, C–F: 1.31, bond angle FCF: 114° ^a	2.239
C ₂ Cl ₄	C=C: 1.38, C–Cl: 1.71, bond angle ClCCL: 116° ^a	2.652

^a Taken from ref 66. ^b Taken from ref 41.

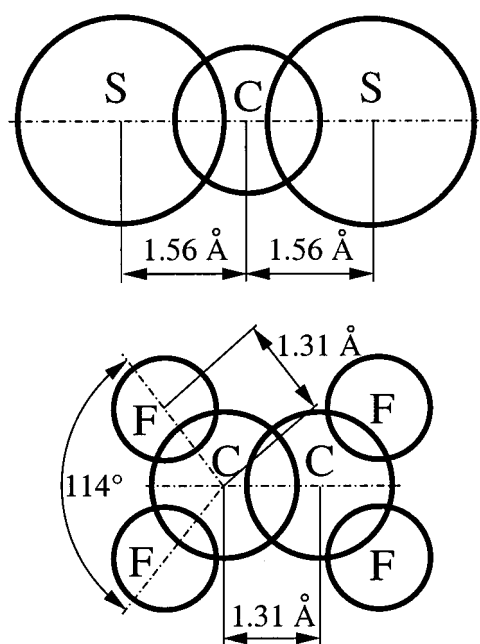


Figure 13. Top: Atom–atom distances in CS₂, cf. Table 6. Bottom: Molecular geometry of C₂F₄, cf. Table 6.

mass. This finding corresponds to the increase of van der Waals radii from top to bottom in the periodic table of elements. For the noble gases and the halogens we also observe an increase of the numbers for ϵ with increasing molecular mass. This

finding corresponds to the empirical rule, that van der Waals dispersion forces increase with the size of the molecule.

5. Conclusions

A consistent set of molecular models for 25 fluids, neon, argon, krypton, xenon, methane, oxygen, nitrogen, fluorine, chlorine, bromine, iodine, carbon dioxide, carbon disulfide, ethane, ethene, ethyne, perfluoroethane, perfluoroethene, perchloroethene, propadiene, propyne, sulfurhexafluoride, tetrafluoromethane, tetrachloromethane, and propylene has been developed. These models, based on the 2CLJQ potential, allow to describe the VLE with an accuracy of about 3% for the vapor pressure, 0.5% for the saturated liquid density, and 2% for the enthalpy of vaporization. The model parameters were obtained from vapor pressure and density data. Predictions of the heat of vaporization and thermodynamic properties in the homogeneous state, also far from the vapor–liquid equilibrium region show good agreement with experimental data. The numbers found for the model parameters show reasonable tendencies and compare favorable to data from other sources such as atom–atom distances. These findings hold promise for successful applications of these models to the prediction of VLE of fluid mixtures.

Acknowledgment. The authors thank Dr. M. Wendland, Vienna, for communicating his synopsis of experimental quadrupole moments and for fruitful discussions. We are grateful to Andreas Linhart for his programming of an inventive software tool for the parameter adjustments. We gratefully acknowledge financial support by Deutsche Forschungsgemeinschaft, Sonderforschungsbereich 412, University of Stuttgart.

References and Notes

- (1) van Gunsteren, W. F.; Berendsen, H. J. C. *Angew. Chem., Int. Ed. Engl.* **1990**, 29, 992.
- (2) Stoll, J.; Vrabc, J.; Hasse, H.; Fischer, J. *Fluid Phase Equilib.* **2001**, 179, 339.
- (3) McLure, I. A.; Ramos, J. E.; del Río, F. *J. Phys. Chem. B* **1999**, 103, 7019.
- (4) Yang, J.; Ren, Y.; Tian, A.-M.; Sun, H. *J. Phys. Chem. B* **2000**, 104, 4951.
- (5) Leonhard, K.; Deiters, U. K. *Mol. Phys.* **2000**, 98, 1603.
- (6) Fischer, J.; Lustig, R.; Breitenfelder-Manske, H.; Lemming, W. *Mol. Phys.* **1984**, 52, 485.
- (7) Shukla, K. *Fluid Phase Equilib.* **1994**, 94, 19.
- (8) Vrabc, J.; Fischer, J. *Mol. Phys.* **1995**, 85, 781.
- (9) Bembek, S. D.; Rice, B. M. *Mol. Phys.* **1999**, 97, 1085.
- (10) Vrabc, J. *Vorhersage thermodynamischer Stoffdaten durch molekulare Simulation*; Fortsch.-Ber. VDI Reihe 3 Nr. 455; VDI-Verlag: Düsseldorf, 1996.
- (11) Jorgensen, W. L.; Madura, J. D.; Swenson, C. J. *J. Am. Chem. Soc.* **1984**, 106, 6638.
- (12) Martin, M. G.; Siepmann, J. I. *J. Phys. Chem. B* **1998**, 102, 2569.
- (13) Chen, B.; Siepmann, J. I. *J. Phys. Chem. B* **1999**, 103, 5370.
- (14) Bohn, M.; Lustig, R.; Fischer, J. *Fluid Phase Equilib.* **1986**, 25, 251.
- (15) Saager, B.; Fischer, J. *Fluid Phase Equilib.* **1991**, 66, 103.
- (16) Lago, S.; Garzón, B.; Calero, S.; Vega, C. *J. Phys. Chem. B* **1997**, 101, 6763.
- (17) Wojcik, M.; Gubbins, K. E.; Powles, J. G. *Mol. Phys.* **1982**, 45, 1209.
- (18) Wang, Q.; Johnson, J. K. *Fluid Phase Equilib.* **1997**, 132, 93.
- (19) Rivera, J. L.; Alejandre, J.; Nath, S. K.; de Pablo, J. J. *Mol. Phys.* **2000**, 98, 43.
- (20) Rodger, P. M.; Stone, A. J.; Tildesley, D. J. *J. Chem. Soc., Faraday Trans. 2* **1987**, 83, 1689.
- (21) Rodger, P. M.; Stone, A. J.; Tildesley, D. J. *Mol. Phys.* **1988**, 63, 173.
- (22) Wheatley, R. J.; Price, S. L. *Mol. Phys.* **1990**, 71, 1381.
- (23) Lísál, M.; Aim, K. *Fluid Phase Equilib.* **1999**, 161, 241.
- (24) Agrawal, R.; Sandler, S. I.; Narten, A. H. *Mol. Phys.* **1978**, 35, 1087.

- (25) Murthy, C. S.; Singer, K.; McDonald, I. R. *Mol. Phys.* **1981**, *44*, 135.
- (26) Murthy, C. S.; O'Shea, S. F.; McDonald, I. R. *Mol. Phys.* **1983**, *50*, 531.
- (27) Fincham, D.; Quirke, N.; Tildesley, D. J. *J. Chem. Phys.* **1986**, *84*, 4535.
- (28) Möller, D.; Fischer, J. *Fluid Phase Equilib.* **1994**, *100*, 35.
- (29) Garzón, B.; Lago, S.; Vega, C.; de Miguel, E.; Rull, L. F. *J. Chem. Phys.* **1994**, *101*, 4166.
- (30) Harris, J. G.; Yung, K. H. *J. Phys. Chem.* **1995**, *99*, 12021.
- (31) Kristóf, T.; Liszi, J.; Szalai, I. *Mol. Phys.* **1996**, *89*, 931.
- (32) Nath, S. K.; Escobedo, F. A.; de Pablo, J. J. *J. Chem. Phys.* **1998**, *108*, 9905.
- (33) Errington, J. R.; Panagiotopoulos, A. Z. *J. Phys. Chem. B* **1999**, *103*, 6314.
- (34) Stapleton, M. R.; Tildesley, D. J.; Panagiotopoulos, A. Z.; Quirke, N. *Mol. Sim.* **1989**, *2*, 147.
- (35) Nosé, S.; Klein, M. L. *J. Chem. Phys.* **1983**, *78*, 6928.
- (36) Potter, S. C.; Tildesley, D. J.; Burgess, A. N.; Rogers, S. C. *Mol. Phys.* **1997**, *92*, 825.
- (37) Pusztai, L.; McGreevy, R. L. *Mol. Phys.* **1997**, *90*, 533.
- (38) Soetens, J.-C.; Jansen, G.; Millot, C. *Mol. Phys.* **1999**, *96*, 1003.
- (39) Gray, C. G.; Gubbins, K. E. *Theory of molecular fluids, Volume 1: Fundamentals*; Clarendon Press: Oxford, 1984; pp 76–85.
- (40) Sados, R. J. *Fluid Phase Equilib.* **1998**, *144*, 351.
- (41) The Chemical Rubber Co. *Handbook of Chemistry and Physics*; 46th ed.; Cleveland, Ohio, 1965.
- (42) Lotfi, A.; Vrabec, J.; Fischer, J. *Mol. Phys.* **1992**, *76*, 1319.
- (43) McGarry, J. *Ind. Eng. Chem. Process Des. Dev.* **1983**, *22*, 313.
- (44) Cibulka, I. *Liquid Density Database*; Prague Institute of Chemical Technology: Prague, 1990.
- (45) Daubert, T. E.; Danner, R. P. *Physical and Thermodynamic Properties of Pure Chemicals (DIPPR-Project)*; Hemisphere Publishing Corporation: 1989, 1991, 1992.
- (46) Stewart, R. B.; Jacobsen, R. T. *J. Phys. Chem. Ref. Data* **1989**, *18*, 639.
- (47) Setzmann, U.; Wagner, W. *J. Phys. Chem. Ref. Data* **1991**, *20*, 1061.
- (48) Reid, R. C.; Prausnitz, J. M.; Poling, B. E. *The Properties of Gases and Liquids*, 4th ed.; McGraw-Hill Book Company: New York, 1987.
- (49) Seidel, P. *Basisdatenbank COMDAB*; Leuna-Werke AG, 1987–1993.
- (50) Jacobsen, R. T.; Stewart, R. B.; Jahangiri, M. *J. Phys. Chem. Ref. Data* **1986**, *15*, 735.
- (51) Schmidt, R.; Wagner, W. *Fluid Phase Equilib.* **1985**, *19*, 175.
- (52) Ely, J. R.; Magee, J. W.; Haynes, W. M. *Research Report-110*; Gas Processors Association: Tulsa, OK 1987.
- (53) Majer, V.; Svoboda, V. *Enthalpies of Vaporization of Organic Compounds*; Blackwell Scientific Publications: London, 1985.
- (54) Friend, D. G.; Ingham, H.; Ely, J. F. *J. Phys. Chem. Ref. Data* **1991**, *20*, 275.
- (55) Jahangiri, M.; Jacobsen, R. T.; Stewart, R. B.; McCarty, R. D. *J. Phys. Chem. Ref. Data* **1986**, *15*, 593.
- (56) Physikalisch-Technische Bundesanstalt PTB—Stoffdatenblätter; Braunschweig and Berlin, 1992–1995.
- (57) Kozlov, A. D. 1996, Moscow. In *REFPROP, NIST Standard Reference Database 23*; Version 6.01, 1998.
- (58) Platzer, B.; Polt, A.; Maurer, G. *Thermophysical Properties of Refrigerants*; Springer: Berlin, 1990.
- (59) Fluid properties from ASMW (Amt für Standardisierung, Messwesen und Warenprüfung der DDR); Berlin, 1985.
- (60) Angus, S.; Armstrong, B.; de Reuck, K. M. *International Thermodynamic Tables of the Fluid State — 7 Propylene*; International Union of Pure and Applied Chemistry; Pergamon Press: Oxford, 1980.
- (61) Möller, D.; Fischer, J. *Mol. Phys.* **1990**, *69*, 463.
- (62) Möller, D.; Fischer, J. *Mol. Phys.* **1992**, *75*, 1461.
- (63) Simmrock, K. H.; Janowsky, R.; Ohnsorge, A. *Chemistry Data Series*, Vol. II, Part 2; DECHEMA: Frankfurt, 1986.
- (64) Wendland, M. *Fluid Phase Equilib.* **2001**, accepted.
- (65) Eubank, P. T. *AIChE J.* **1972**, *18*, 454.
- (66) Landolt-Börnstein, *Zahlenwerte und Funktionen aus Physik, Chemie, Astronomie, Geophysik und Technik*, Board I/2, 6. Aufl.; Springer: Berlin, 1961.